Heliyon 9 (2023) e12983

Contents lists available at ScienceDirect

Heliyon

journal homepage: www.cell.com/heliyon

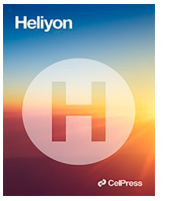

Research article

The effect of water-to-binder ratio (W/B) on pore structure of one-part alkali activated mortar

Eddy Yusslee *, S. Beskhyroun

Auckland University of Technology (AUT), Auckland, 1010, New Zealand

ARTICLE INFO

Keywords:
Microstructure
Scanning electron microscope (SEM)
Dispersive X-Ray analysis (XRD)
Calcium oxide (CaO)
Superplasticizer (SP)

ABSTRACT

One-part alkali-activated materials (AAMs) are alternative cementitious materials to respond to the shortcoming of conventional two-part systems. Combining aluminosilicate precursor by-products with ordinary Portland cement (OPC) helps develop a robust performance. It can potentially be used as a patching product for concrete repair materials.

Mix design for the one-part AAMs in this report is formulated to ensure its application is according to the structural concrete repair materials Class R4, EN1504-3 specification. In addition, the lower alkalinity alkali activator employed is helpful for economic reasons and less harmful to handle. Furthermore, the addition of powdered admixture enhances the performance of hardened products for retarding effect, provides additional calcium for geopolymer reactions, and offers stable mechanical strength. Finally, an adequate water-to-binder (W/B) ratio has completed the mix design proportion and effectively activated the chemical reaction of the dry mixed ingredients in the geopolymerization process for binding purposes.

In this study, the water-to-binder ratio was set in the range of 0.30, 0.35 and 0.40 for all mortar samples at constant mix design formulation and activated by low alkalinity of solid potassium carbonate (K_2CO_3). At 0.30 W/B ratio, the setting time is delayed to 120 min but shorter than other W/B ratios. Mechanical strength of the mortar increased over time up to 63 N/mm^2 at 56 days of curing age, recorded low porosity level of 16%, minimal pore structure area of 17.374 m^2/g and documented above 2.0 MPa of pull-off bonding strength that encounters restrained drying shrinkage and expansion impact at 56 days of age under different curing conditions.

1. Introduction

Alkali-activated materials (AAMs) are synthesized from solid aluminosilicate precursors and alkali activator reactions. They become greener alternative cementitious materials to the traditional ordinary Portland cement (OPC) [1]. The AAMs technology does not require clinker for cement hydration products. In contrast, the excessive energy consumption required for clinker up to 5 GJ per ton is needed to burn limestone and silicious materials to manufacture clinker [2]. OPC emits tons of CO_2 that contributes up to 7% of greenhouse gas emissions resulting in global warming and climate crisis [3]. Therefore, industrial by-products in AAMs were introduced as a partial substitute for OPC cement for construction purposes. Conventional AAMs are produced with two products: solid aluminosilicate precursors and the aqueous solution of alkali activators. A higher alkalinity level is required to ensure the best performance of the cementitious products, although it means costly besides consists of highly corrosive chemicals that might risk the

* Corresponding author.
E-mail address: eddy.yusslee@aut.ac.nz (E. Yusslee).

https://doi.org/10.1016/j.heliyon.2023.e12983
Received 2 September 2022; Received in revised form 8 January 2023; Accepted 11 January 2023
Available online 14 January 2023

health and safety of the worker. Nevertheless, using a viscous aqueous activator makes it sticky and prevents it from an extensive in-situ application on the construction site. Therefore, the alkaline solution is replaced with a dry alkali activator in one-part AAMs technology for more practical applications.

However, without relevant formula, the one-part AAMs have some significant drawbacks on their long-term durability from the perspective of microstructural and nanostructural levels, which further affect the mechanical strength and durability, causing this type of geopolymer binder is still not famous for a commercial adaption at present [4]. Many reports have been established on the development of one-part AAMs. Fly ash consists of high silica content beneficial to improve the reaction rates in the geopolymerization process. However, it has low calcium, preventing it from strengthening the *C*–S–H gels for binding products. Adding calcium-rich slag filled the shortage by supplying additional calcium. Combining these two precursors creates an additional 3D network of *N*-A-*S*-H gels that co-exist with *C*-A-*S*-H gels from the main parent product of *C*–S–H [5,6]. The FA/GGBFS precursors exhibited higher mechanical strength in one-part AAMs in concrete. However, too high GGBFS content will cause rapid hardening, water loss and higher shrinkage. Thus, OPC, which has a significant amount of calcium, was added in one-part AAMs as part of the precursors. OPC has been widely used as concrete and cementitious mortar. Still, with the presence of by-product precursors, the dependency on the OPC can be reduced, indirectly cutting down its volume. Askarian et al. [7] explained on one-part AAMs activated with the combination of by-product precursors and OPC in concrete can achieve up to 55.0 MPa with 60% of OPC content at 28 days of curing age. However, its mechanical strength in the form of repair mortar is still not yet established. Luukkonen et al. [8] reviewed past studies on hybrid one-part AAMs performance and found that it has higher mechanical strength subject to a different percentage of OPC inclusion. The report comprises a few studies, including a 60% OPC mixed with 40% fly/bottom ash, which has recorded 32 MPa compressive strength at 28 days of curing age but has a higher W/B ratio of 0.5 and a tendency towards shrinkage. In addition, 20% OPC/40% GGBFS and 40% kaolin/bentonite mixtures recorded compressive strength with promising 32 MPa at 28 days of age but had inconsistent W/B ratio of 0.3/0.5 besides being triggered with slightly higher alkali activator (5% solid sodium carbonate). Solid sodium hydroxide was used to activate the mixed precursor composed of OPC/FA/kaolin has an efflorescence effect due to the lower reactivity that causes some sodium to be replaced by calcium. Nevertheless, this hybrid AAMs has recorded sufficient 27 MPa compressive strength (at 28 d). Moreover, in this review report, a patented geopolymeric cement containing 3–30% OPC has been tested at 28 days of age and recorded 35 MPa (30% OPC) of compressive strength. However, the pore structure of the hardened cement for all 43 patented dry mix cement compositions samples was not reported, making its durability uncertain.

In addition, minimal study on the effect of low alkaline activators is used to activate the one-part AAMs cementitious materials because higher alkalinity is more significant to complete the geopolymerization process to produce standard quality cement binder. Excessive alkalinity, on the other hand, causes significant drawbacks to the pore structures of the hardened products and is prone to chemical attacks in a harsh environment. Yang et al. [9] mentioned that the slag paste was activated with a 15% sodium carbonate alkali activator has demonstrated a bigger pore diameter and pore volume than a 10% sodium carbonate, suggesting an excessive alkali activator could be coarse in the pore structures. Another study reported by Azevedo et al. [10] proved that with a higher dosage of alkali activator, the average pore diameter decreased from 24.29 nm to 21.48 nm and documented higher compressive strength up to 41 MPa at 28 days, subsequently supporting the fact that the elevated concentration of alkali activator encourages the hardened product to be more dense and solid without decreasing any unreacted particles.

Still, it has also affected the porosity between 30 and 40% for one-part AAMs composed of calcined commercial kaolin and ceramic waste. Gel pores and capillary pores are two significant matters in the strength of cementitious products where gel pores are unlikely to affect much strength properties but are reported to be influential on creep and shrinkage [11]. However, not all finer pores are harmful. There are four ranges of pore sizes that influent the compressive strength of hardened AAMs, which are classified as harmless pores for sizes below 20 nm, less harmful pores for 20–50 nm, harmful pores if 50–200 nm and more harmful pores if exceed 200 nm [12]. It was reported that two-part AAMs composed with a single metakaolin precursor used as concrete repair materials recorded 2.0 MPa maximum bond strength, but 20% replacement with slag showed an increment in pull-off bonding strength as an indication of mixed aluminosilicate precursors exhibits greater strength than a single type of binder precursor source. Both compositions have documented about 14% porosity level [13].

A fully reacted microstructure pattern on the surface could be formed by increasing the alkali activator in a dry mixture, as reported by Ref. [10]. Yet, excessive alkali content in the mixture can migrate to the surface and react with CO_2 in the atmosphere, consequently causing carbonation. The use of hybrid one-part AAMs concrete studied by Ref. [7] explained that the inclusion of 30% OPC in the mixes has more compact microstructures and less unreacted fly ash particles compared to 0–20% of OPC content but has a more porous structure than 40% and 60% of OPC content. In that report, the compressive strength for one-part AAMs concrete with 60% OPC was about 55.0 MPa. In comparison, adding 40% OPC and 30% OPC in one-part AAMs concrete composed with a single precursor of metakaolin recorded compressive strength of about 52.0 MPa and 50.0 MPa at 28 days of age, which was activated by 3–5% of alkali activator. It is worth mentioning that one-part AAMs composed of single precursors of metakaolin promote a highly porous structure, heterogeneous with unreacted particles that affect its mechanical strength and durability as illustrated in SEM images [14]. In contrast, one-part AAMs composed of two aluminosilicate precursors of fly ash and slag have denser microstructure than fly ash only mixes to confirm that combination of aluminosilicate precursors contributes better mechanical strength, rich in Al but has a substantial low Ca/Si ratio which the hydrated OPC has the advantage to offer a higher Ca/Si ratio and compensate this shortage [15].

At the current stage, one-part AAMs technology mainly focuses on concrete product purposes as an alternative option to the conventional OPC based cementitious. One-part AAMs mortar is to be developed to reduce dependency on OPC mortar and be comparable to other mortar repair materials in the market. Combining more than one precursor was designed to be mixed with the OPC as an initial approach towards promoting green and sustainable construction materials by utilizing industrial by-products as the primary aluminosilicate precursors source and cutting down the volume of OPC as low as it can be. Furthermore, a lower dosage of the

solid alkaline activator is beneficial for a cheaper cost, lower health risks and is not harmful to the environment. First, the effect of a low alkaline activator used in one-part AAMs must be observed on its reaction with main precursors. For this reason, the water-to-binder effect will support the geopolymerization process before conducting a microstructural study to deliver more understanding of the mechanism of its physical property's behaviour. Yusslee et al. [16] reported that the one-part AAMs' mechanical strength has compressive strength and pull-of bond strength level that complied with Class R4-EN1504-3 standard, indicating the potential of this type of geopolymer binder to be used as concrete patch repair mortar. However, the constancy of pore structures of the hardened mortar has yet to be proved; thus, its durability stays doubtful.

It is crucial to understand how pores start created during the hardening process as the water content difference affected the hydration products and strength development. Many researchers activate dry mixtures for one-part AAMs application with different W/B of ratios [7,10,15]. Luukkonen et al. [8] reported that in one-part AAMs, four steps occur after water is added to cementitious materials, beginning with ion exchange, hydrolysis, network breakdown and release of Si and Al, which differentiate the one-part technology from the conventional two-part AAMs. It is worth mentioning that as the geopolymerization cycle continues, the cracks and pores formed at the early stage were filled with an increasing amount of gels and justify compressive strength development over time as the result of a reduction in the accumulated volume of the pores, mainly from *C*-A-*S*-H gels phase fill the pore structure to reduce the pore diameter [9,17]. The compressive strength of one-part AAMs containing fly ash, OPC and slag as the main component reacted with an alkali activator to produce gel formation of sodium aluminosilicate hydrate (*N*-A-*S*-H), calcium alumino-silicate hydrate (*C*-A-*S*-H) and stable 3D network of silico-aluminate structures that enhance polycondensation process that contributes to the higher compressive strength [18].

The addition of commercial solid additives will be added and formulated in the one-part AAMs dry mixtures to control and stabilize the hardened products of mortar. The inclusion of lignosulfonate (LS) type superplasticizer (SP) as high range water reducing admixtures improved the dissolution of slag and reduced water content for better mechanical properties [19,20]. At the same time, the addition of OPC and CaO powder provided more calcium. As a result, it increased the compressive strength on the effect of water content for high compressive strength of AAMs cementitious products [19]. Differences in SP effect on one-part AAMs depend much on the stability behaviour of admixtures in a different type of solid activator. Quicklime-type of Calcium Oxide (CaO) was used as an expansive agent in mortar. Adding the CaO with Shrinkage Reducing Admixture (SRA) has increased the mortar volume instead of shrinking it like conventional cementations materials. Hence, the initial impression on the selection and composition of solid admixtures for the mix design of this study was based on the above findings and the previous study by Ref. [16].

Undeniable, the one-part AAMs have become a popular option in the form of concrete. Current studies largely focus on the synthesis and characterization to determine the new type of precursor-green products. Researchers utilize various types of waste products from agriculture and construction on top of traditional industrial by-products, fly ash, slag and metakaolin [21,22,23,24]. However, the engineering application for the one-part AAMs in other cementitious-based materials has still lagged. On the contrary, mortar composed of two-part AAMs systems has been tested as concrete repair products and reported to have great potential to be commercial in the construction industry [25,26]. The one-part AAMs must be developed not only to focus on their compressive strength but must have robust physical structures, higher consistency and be chemically stable.

The motivation to carry out this study is to analyze further the fact that the higher water content could decrease the yield stress and plastic viscosity of fresh cementitious materials and affect their rheology behaviour and performance at the hardened stage [27]. Nevertheless, the water content in the water-to-binder (W/B) ratio can be adjusted to change yield stress and plastic viscosity. Still, in actual construction, the W/B are conventionally controlled to ensure homogeneity of the mortar or concrete, besides operated practical handling from mixing and transporting to pouring time. Moreover, unlike the conventional one-part AAMs, which traditionally utilize industrial waste or/with natural pozzolanic materials as main aluminosilicate precursors [28], hybrid one-part AAMs, on the other hand, combine the industrial by-products with the OPC used as the main source of the cementitious binder in this study [7,8].

Therefore, the objective of this study is to examine the effect of W/B content on the pore structures of fly ash/slag precursors mixed with the OPC for repair mortar application. This study aims to reduce the porosity level of one-part AAMs by controlling the pore structure size of the hardened mortar with appropriate water content and safeguarding its mechanical strength against shrinkage effect after 28 days of curing age for concrete patching mortar application. Consequently, the hybrid one-part alkali-activated mortar in this study was activated by different W/B ratios of 0.40, 0.35 and 0.30 to encounter previous findings, which stated that alkali-activated materials exhibit higher porosity levels and larger pose size than those reported in ordinary Portland cement (OPC), hence by controlling W/B ratio, it could produce less porous polymeric microstructure [29]. Thus, the optimum W/B ratio will complete the novel contribution of a new mix design formulation for Class R4 - EN1504-3 standard for structural concrete repair mortar application previously developed by the author [30]. Furthermore, the hybrid one-part alkali-activated in this study was activated with low alkalinity of solid alkali activator as part of the research in developing sustainable cementitious product technology by the author for engineering application.

This new type of repair mortar could efficaciously reduce clinker cement production and mitigate the carbon footprint linked to the construction industry. Furthermore, the reported result from this study will stipulate the prerequisite of understanding the interrelationship between compositions of solid materials ingredients with their physical properties when water reacts with a dry mixture of precursors, activators, aggregates, and admixtures (dissolution process of solid particles).

2. Materials and method

The experiment conducted in this report used three main aluminosilicate precursors: Fly Ash Class-F as per ASTM C618, Ground Granulated Blast Furnace Slag as per ASTM C989 and ordinary Portland cement (OPC). A powdered Potassium Carbonate (K2CO3,

purity ≥90%) was used as the sole alkali activator. First, three solid admixtures were added to the mix design formulation: sodium lignosulfonate as a superplasticizer additive (SP), shrinkage-reducing admixture (SRA) – commercial ethylene glycol type, and calcium oxide power (CaO). Both SRA and CaO control the effect of drying shrinkage of the mortar. Next, natural sands were added to increase the mortar volume and source of additional calcium with a specific gravity of 2.67 and has an average particle size (D50) of 90.23μm. Finally, water is added to activate the mortar mix for testing in a fresh and hardened state. The chemical compositions of fly ash, slag and ordinary Portland cement are shown in Tables 1–3, respectively. In addition, the particle size for each material is measured with the Laser Diffraction Analysis (LDA) and elaborated in Table 4. This report's materials and mix design formulation were according to the author's previous study in developing novel mix design formulation for one-part alkali-activated mortar used as structural concrete repair materials [16,30].

a. Mix proportions

This study aims to reduce the porosity level of the one-part AAMs mortar by analyzing the pore structures of the structural repair mortar activated with one-part AAMs technology at three different water content levels of 0.40, 0.35 and 0.30 water-to-binder (W/B) ratio. Samples were marked with G1 composed with the highest W/B ratio of 0.40 (high water content), G2 has a W/B ratio of 0.35 (medium water content), and G3 has the lowest W/B ratio of 0.30 (low water content). Sample G1 was selected as the control sample in order to compare the pore structure behaviour if the W/B is decreased and its influence on determining the workability in the fresh state, mechanical strength and durability in the hardened state. Three admixtures were added in the mix design with a constant proportion of 0.30% of SRA, CaO (0.15%) and 1% SP from total aluminosilicate precursors weight. The sand content was fixed at 1 (binder/aggregate ratio) for all samples. The mix design formulation of the mortar is shown in Table 5. All samples were cured under controlled temperature per EN1504–3:2005 standard, part 3: structural and non-structural concrete repair materials.

b. Sample Preparation

Dry mixtures of FA, GGBFS, OPC, SP, SRA, CaO and fine aggregates were blended for 2 min using an electric mixer (EX-EM2000 EXTRAMAN, 2000W). Next, water was added to the mixtures and blended for 3 min until the mortar paste was uniform. Finally, the fresh mortar the filling into the 40 mm × 40mm ×160mm steel moulds for the compression strength test and vibrated for 2 min and dismantled form moulds after 24 h. All samples were cured under the lab-controlled temperature of 20 ± Celsius and relative humidity of RH > 90% before being tested at the 7th, 28th and 56th days of age. The experiment on the cementitious paste was done without aggregates using Vicat moulds for the penetration process to check its consistency. The setting time measurement and pull-off bonding strength test also used similar temperatures and RH. Additionally, the flow table test was carried out under lab temperature of 29–30 Celsius and RH between 55 and 60%. For this test, the fresh mortar was filled and compacted into truncated conical moulds at the flow table platen before jolting the samples.

c. Experimental and procedures

A compression strength test machine, AUTOMAX5, was used to determine the compressive strength of hardened mortar at the 7th, 28th and 56th days of age with an applied loading rate of 2.4 ± 0.2 kN/s. Samples were produced in triplicate for each test, and the mean value of three readings was taken as the final strength value. Setting time cement paste was set for 120 min as the first interval time. The Vicat moulds used are 40 ± 0.2 mm in height, and the first setting time is recorded when the penetration depth of 34 ± 3 mm is obtained, while for final setting time, it is recorded when 0.5 mm penetration depth is achieved to comply with EN 196–3: 2016 standard. For the flow table test, after the truncated conical moulds are removed, the flow table is jolted 15 times and measured using a calibrated calliper. The average of two spread dimensions was recorded to get the flow value according to BS EN 13395-1-2002 standard. To examine the shear strength and tensile strength level, the pull-off test is carried out by means of determining restrained drying shrinkage or expansion impact after the hardening process stops at 28 and 56 days of curing age under three different curing conditions as per EN 12617–4 test method as part of the durability checking in EN1504-3 guidelines. Analyzing pore structural characterization, crushed samples from mechanical strength tests were used and measured with Mercury Intrusion Porosimetry (MIP) using a MicroActive Autopore V9600 machine. Scanning Electron Microscope (SEM) and Energy Dispersive X-Ray analysis (EDX) were employed to analyze micromorphological features and elemental compositions of the mixes in the form of hydrated particles. The SEM scanned the fractured mortar surfaces at 28 days of age while the EDX (BSE/20 KV) observed the elemental composition in the samples.

Table 1
Chemical compositions (%) of Fly Ash obtained from XRF analysis.

Chemical Composition	Percentage (wt %)	Chemical Composition	Percentage (wt %)
SiO_2	55.94	**TiO_2**	0.72
Al_2O_3	22.60	**Cr_2O_3**	–
Fe_2O_3	8.10	**MnO**	–
CaO	6.26	**SO_3**	1.02
P_2O_5	0.36	**LOI**	1.48
MgO	1.21	**Cl**	0.03
K_2O	1.66	**Na_2O**	0.62

Table 2
Chemical compositions (%) of Ground Granulated Blast Furnace Slag (GGBFS) obtained from XRF analysis.

Chemical Composition	Percentage (wt %)	Chemical Composition	Percentage (wt %)
SiO_2	35.91	**TiO_2**	0.59
Al_2O_3	16.56	**Cr_2O_3**	–
Fe_2O_3	1.52	**MnO**	–
CaO	35.28	**SO_3**	0.36
P_2O_5	0.36	**LOI**	–
MgO	6.01	**CI**	–
K_2O	–	**Na_2O**	1.76

Table 3
Chemical composition (%) of Ordinary Portland Cement (OPC).

Chemical Composition	Percentage (wt %)	Chemical Composition	Percentage (wt %)
SiO_2	23.97	**MgO**	1.36
Al_2O_3	5.27	**K_2O**	0.51
Fe_2O_3	3.28	**TiO_2**	0.06
CaO	60.12	**SO_3**	2.20
Na_2O	0.23	**LOI**	2.00

Table 4
Laser Diffraction Analysis (LDA) measured the particle size distribution.

Samples	D10 (μm)	D50 (μm)	D90 (μm)
FA	2.682	14.08	54.92
GGBFS	2.819	19.99	57.25
OPC	2.690	16.32	47.96
K_2CO_3	299.1	448.4	645.6
SRA	2.334	12.81	35.20
CaO	1.728	4.949	20.61
SP	16.12	35.88	56.86
Sand	11.16	92.95	220.8

Table 5
Mix design ratio for one-part alkali-activated mortar.

Samples	Binder			Alkali activator	Solid admixtures			Design ratio	
	FA (%)	GGBFS (%)	OPC (%)	K_2CO_3 (%)	SRA (%)	CaO (%)	SP (%)	Binder/Sand	Binder/Water
Mix G1	25	5	70	1.60	0.30	0.15	1	1	0.40
Mix G2	25	5	70	1.60	0.30	0.15	1	1	0.35
Mix G3	25	5	70	1.60	0.30	0.15	1	1	0.30

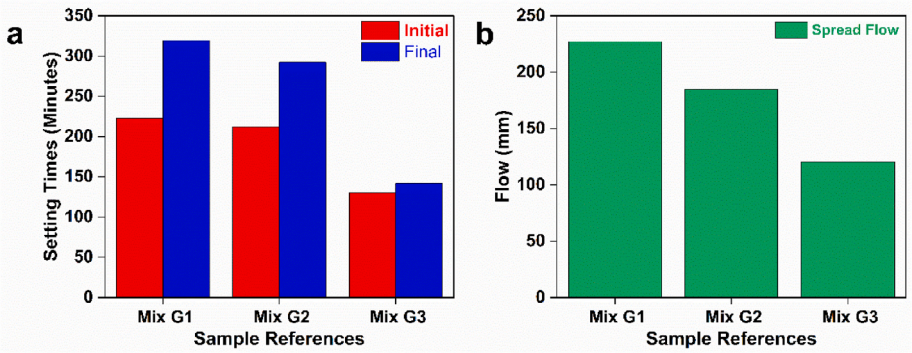

Fig. 1. Setting time and workability test result of one-part AAMs mortar (paste samples).

3. Result and discussion

3.1. Setting time and workability test

The workability of the one-part AAMs mortar determines by observing how easily the fresh mortar deforms when stress is applied. Fig. 1a above shows that sample Mix G3, activated by the water-to-binder (W/B) ratio of 0.30, has the shortest initial and final setting time, followed by sample Mix G2 and control samples Mix G1. All cement paste samples recorded more than 2 h (>120 min) of initial setting time but what makes them different is low water content effectively expedited the final setting time to 142 min for cement paste sample G3 compared to mortar samples G1 and G2, which have recorded much longer time above 290 min (>4 h). An extended initial setting time in this result as a result of a low alkaline medium delayed the chemical reaction and geopolymerization process, contrary to the higher activator content, which has a more rapid reaction for a faster setting time. Furthermore, the inclusion of superplasticizer (SP) also has a retarder effect on the development of hardened mortar attributed to the adsorption properties of SP on the precursors material particles of FA, slag and OPC, as documented by [20].

Nevertheless, in this study, water content was the main factor differentiating between all paste samples. The lower W/B ratio can shorten the setting time due to heat generation from solid activators when reacted with water. Askarian et al. [7] found that the paste only contained FA and GGBFS and failed to harden in 24 h but recorded the shortest setting time by incorporating 60% OPC in the mixes. However, a short setting time could prevent proper casting at the construction site besides transporting issues from the batching plant. As for the flow table test, the higher water content in sample Mix G1 spread up to 227.24 mm makes it less viscous because of excess water compared to the samples with lesser water content, Mix G2 (184.95 mm) and G3 (120.40 mm) as shown in Fig. 1b. These findings represented a 47% reduction in mortar spreading capacity when the W/B ratio of 0.40 was reduced to 0.30. It is worth noting that the finer the particles are, the lower the spreading flow is [12]. Though all mortar samples were spread firmly, no segregation was found on the flow table. This trend also confirmed the roles of CaO as one of the admixtures used in mix design which favoured the formation of homogeneous materials, low viscosity and reduced segregation of fresh materials [28]. The workability of the mortar is beneficial when applied as a repair patching material to ensure the patched mortar remains firm, set, and bonded well on a substrate. Nevertheless, the W/B ratio has influenced cementitious mortar's yield stress and plastic viscosity. When cement particles come into contact with water, it begins to dissolve and are hydrated. Positive and negative charges will occur because of this reaction, encouraging electrostatic activities among cement particles and leading to the flocculation of the particles. Finally, cement particles absorb the amount of water, and as a sequence, the free amount of water will be diminished, leading to a higher content of solid volume fraction. As a result, yield stress and plastic viscosity level will subsequently rise, which improves the workability of the fresh one-part AAMs mortar [27]. In this study, the lower water content of the W/B ratio of 0.30 delayed the hardening process (low plastic viscosity) but was shorter than the W/B ratio of 0.35 and 0.40. Higher yield stress and lower plastic viscosity ensure the fresh mortar is more stable and flows consistently, but too viscous could be a disadvantage if applied as sprayable mortar as it is not easy to be pumped out from the pipe. On the contrary, lower W/B with higher slag content also reported a setback in autogenous shrinkage and cracking [18] due to its porosity and pore size reported larger than the OPC [29], which is further discussed in the later section in this report.

It can also be concluded that with the optimum water-to-binder ratio of 0.30, the reaction between precursors (composed with only 70% OPC content) with low alkaline activators as main synthesized products can lengthen the one-part AAMs setting time within an acceptable allowable range that beneficial for mixing, transporting, and pouring operation at the site.

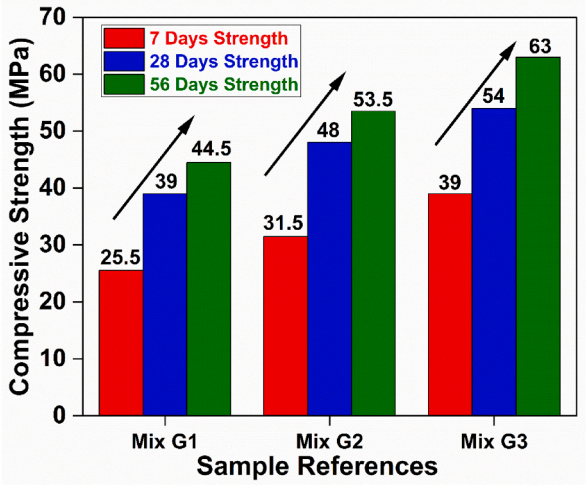

Fig. 2. Compressive strength result for mixed one-part AAMs repair mortar at 7, 28 and 56 days of curing age.

3.2. Compressive strength test

Compressive strength development for all mortars increases with time regardless of the water-to-binder (W/B) ratio, illustrated in Fig. 2. Mortar sample Mix G3 has recorded higher compressive strength for all curing periods beginning at 7 days of curing age and continues to develop later. Mortar sample Mix G3 has recorded the highest strength at 54.0 MPa, followed by mortar sample Mix G2 with 48.0 MPa and sample Mix G1 with 39.0 MPa at 28 days of age. Both mortar samples, Mix G2 and Mix G3 recorded above the minimum requirement for class R3 and subsequently met the class R4 - compressive strength standard as per EN1504-3 specification. At lower alkaline medium, mortar sample G3 managed to record the highest compressive strength at 63.0 MPa, followed by samples G2 and G1 at 53.5 MPa and 44.5 MPa, respectively, at 56 days of curing age.

The W/B ratio significantly influences cementitious materials for proper workability and strength. This result confirmed that the lower the W/B ratio, the higher the hardened mortar's compressive strength. Moreover, the lower binder-to-aggregate ratio used in this study was set to 1, beneficial to acting as reinforcement in the matrix and providing high dimensional stability to the mortar, improving mechanical performance and adherence level [31]. Apart from that, the compressive strength of one-part alkali AAMs product in this experiment keeps increasing after 28 days of age and confirms the geopolymerization process remains in force.

The use of a low W/B ratio of 0.30 successfully reduces the water content and has improved the compressive strength in line with the findings on the compressive strength development is correlated with the fine and large pore's diameter [20]. To understand it better, this report's latter part investigates the compressive strength result from the pore structure perspective. The inclusion of a

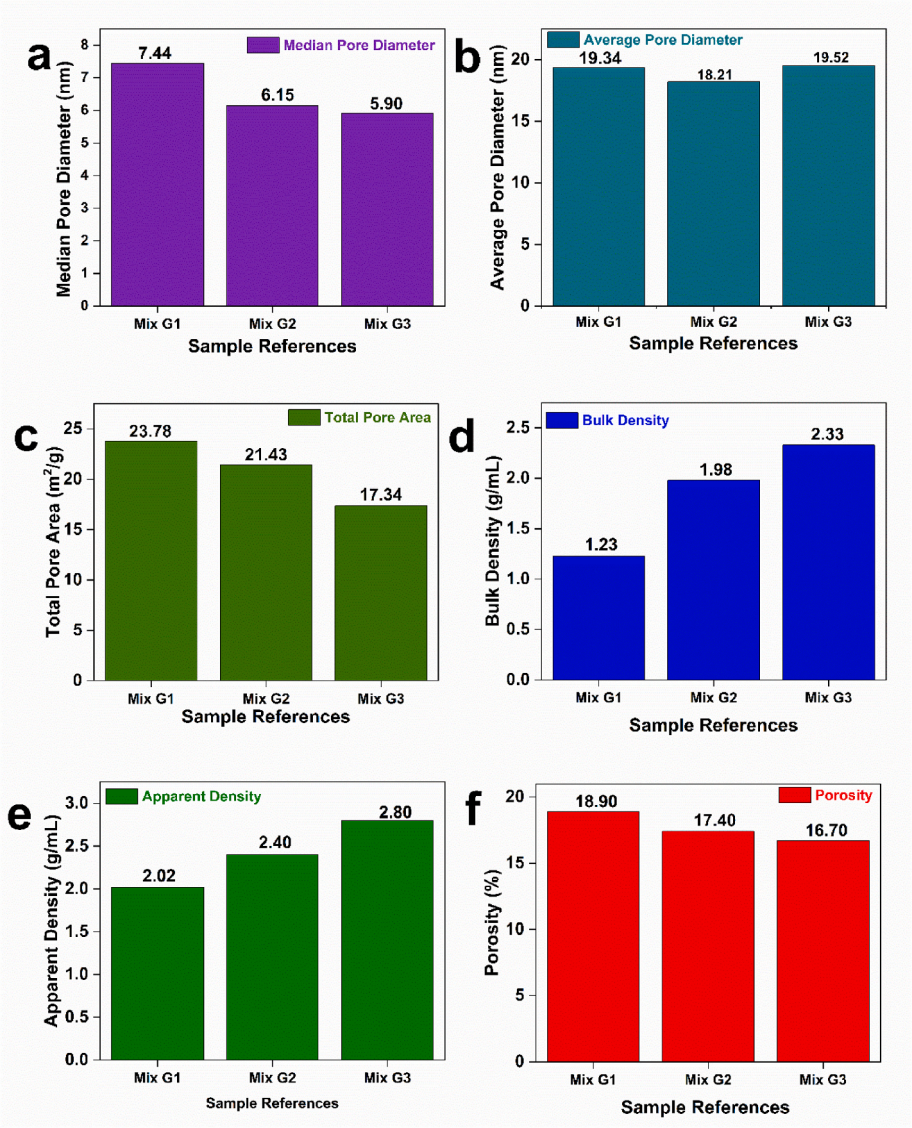

Fig. 3. Pore structure distribution of hybrid one-part alkali-activated mortars.

combination shrinkage-reducing admixture (SRA) and CaO – expansive agent contributed to the higher compressive strength for mitigating shrinkage by reducing the surface tension of pore water and micropores. When water is added, the SRA helps decrease internal stress during evaporation, while CaO counteracts the shrinkage's effect by reducing the capillary stress. The porosity level, however, can be controlled by diminishing the capillary stress of the water generated by SRA during the mortar mixing process, although the usage of ethylene-glycol-based admixture reported has a setback in affecting the elasto-mechanical properties [32]. The expansion of mortar is extended with the addition of CaO during the hydration process and only starts to shrink when the wet curing is stopped. The combination of CaO and SRA reported gave a better performance concerning the cracking resistance of the mortar due to the shrinkage effect, which is valuable for better mechanical properties of hybrid one-part AAMs [33].

3.3. Pore structure analysis

Pore structure distribution of mortar samples Mix G1, G2 and G3 were analyzed with Mercury Intrusion Porosimetry (MIP). The results are shown in Fig. 3a - f. The mortar specimens were collected from the crushed cube samples from the 28-d compressive strength test. The median pore diameter is mainly distributed between the range of 5.90 nm–7.44 nm (Fig. 3a). The average pore diameter for all mortar samples has no significant difference and is measured at 19.34 nm, 18.21 nm, and 19.52 nm for mortar samples G1 (W/B of 0.40), G2 (W/B of 0.35) and G3 (W/B of 0.30), respectively (Fig. 3b). It is worth noting that pores sizes in the range of 3.5–10 nm are commonly described as small gel pores type, while 10–100 nm are better known as large gel pores [1], 50 nm–10 μm as capillary pores that cause detrimental to the strength of hardened samples and voids if the pore size is more than 10 μm [17]. However, voids or air bubbles have less impact on the strength during the sample preparation process triggered by vibration or mould defects [34]. Gel pores size found in this experiment as a sign of the complete reaction process of the products that can fill capillary pores with the addition of slag may decrease polymerization degree and improve pore size distribution of the mixes and strength development as reported by Ref. [15].

The increase in porosity percentage will also reduce mechanical strength performance on the one-part AAMs [10]. The sample Mix G3 has an overall better pore structure distribution in terms of a low total pore area of 17.374 m^2/g (Fig. 3c), higher density of 2.33 g/mL (Fig. 3d), smaller median pore diameter (Fig. 3e) and as a result, Mortar G3 has a low percentage of porosity of 16.655% (Fig. 3f), compared to mortar sample Mix G2 and G1.

This contributed to the inclusion of the OPC able to decrease microstructure porosity with the formation of amorphous Ca–Al–Si gels [7] and was discussed further in this report's SEM images analysis section. In comparison to other one-part AAMs, Samarakoon et al. [11] reported that the porosity level for one-part fly ash/slag-based materials was 35.96% (activated by sodium silicate/sodium hydroxide solution), 39% porosity (activated by soda lime glass powder/sodium hydroxide) and 29% porosity activated by solid sodium silicate. On the other hand, for two-part AAMs, Kramar et al. [35] stated that a higher porosity level was recorded for metakaolin-based mortar (16.5%) followed by fly ash mortar (13.2%) and slag mortar (11.1%). As published in the report, it is interesting to note that only metakaolin-based mortar has complied with the class R4 standard and class R3 standard for fly ash-based AAMs, as per EN1504-3 specifications. However, a larger range of average pore diameter between 20 and 140 nm detected in two-part AAMs mortar samples in that report compared to the mortar samples in this study showed that the introduced hybrid one-part AAMs has not only improved the existing one-part AAMs performance but also comparable to the two-part AAMs system for concrete repair application.

Furthermore, the total pore area occupied under controlled lab temperature curing mortar at a W/B ratio of 0.35 is 23.778 m^2/g but significantly reduced to 17.374 m^2/g for mortar samples with a W/B ratio of 0.30. A 26% decrease in porosity is contributed to the enrichment of pore structures as an effect of the dense and compact hybrid one-part alkali-activated mortar where the group of

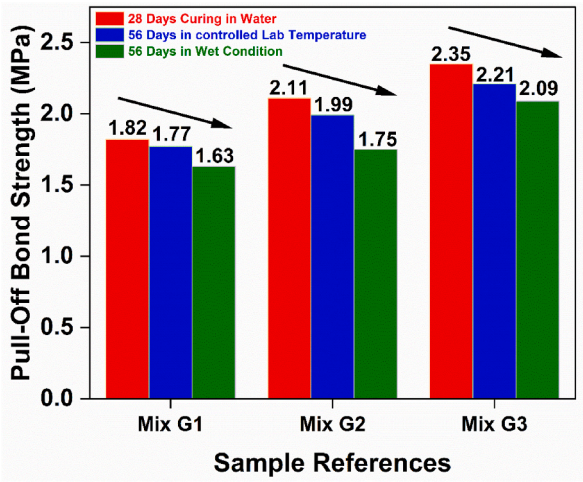

Fig. 4. Restrained drying shrinkage behaviour (pull-off bond strength result).

aluminosilicate *C*-A-*S*-H gels characterized the geopolymer matrix *Si*–*O*–Al network that reflects porous fundamental structure in geopolymerization process to refined the pores [17]. The ongoing alkali activation at a later stage encourages more pore structure refinements, contributing to the better compressive strength performance for samples Mix G2 and Mix G3 at 28 days in this report. On the other hand, one-part AAMs activated by the dry activator of NaOH micro-pearls powder have a coarser pore fraction of more than 20 nm at a W/B ratio of 0.1 and subsequently prone to chemical attacks and potentially lower resistance against severe curing conditions than two-part AAMs counterparts [11]. Contrary, findings from this report indicate that a lower dosage of potassium carbonate reacts well with the optimum water-to-binder ratio of 3.0 in the geopolymerization process, capable of refining the pore size of the mortar by filling the capillary pores, subsequently increasing the degree of microstructure densification and justified the higher compressive strength result in this report.

3.4. Restrained drying shrinkage and expansion

The hybrid one-part alkali-activated mortars continue to be tested to determine their shrinkage impact by conducting a pull-off bond strength test under three different curing conditions between 28 days and 56 days of age as per EN 12617–4 test method. The pull-off bond strength trend for all mortars declines over time for all mortar samples, as shown in Fig. 4 and confirms that each mortar sample was shrinking after the hydration process was completed or drying (loss) of capillary water/moisture for curing. When hardened mortar shrinks, tensile stress increases, leading to cracking and other internal deforming, thus affecting its homogeneity and compactness. Consequently, the shear and tensile bond strength of the hardened mortars at repair and the concrete substrate surface will be weakened and influence the adhesion interface. Mortar samples cured for 28 days were soaked in the water as control values showed the highest pull-off bonding strength for each mixed sample, followed by 56 days curing under lab temperature, and 56-day wet curing condition (wrapped with water bath) was the lowest pull-off bonding strength amongst all. It is interesting to understand that pull-off bond strength for mortar sample G3 activated with a W/B ratio of 0.30 has recorded above 2.0 MPa for all curing conditions and thus complied with the Class R4 ($\geq$2.0 MPa) while both mortar samples G1 and G2 even though recorded pull-off bond strength >1.5 MPa, they were only satisfied the Class R3 standard. It is vital to note that the pull-off bond strength of control values for mortar samples G3 only dropped slightly to its lowest recorded strength (−2.55%) compared to its counterpart, G1 (−10.44%) and G2 (−17.06%) and explain on the little effect of internal stress because of low shrinkage level. It does not affect the shear and tensile strength of the hardened mortars, indicating higher adhesive force [16]. The result of this experiment was in good agreement with the fact that the lower alkali activator dosage will have lower shrinkage and thermal effects on the hardened samples [36]. It also confirmed water content's vital role in controlling porosity levels in limiting drying shrinkage in alkali-activated materials systems.

The correlation between the porosity level of one-part AAMs mortar and mechanical strength before and after hardened mortar shrink at 56 days of curing are shown in Fig. 5 above. At the constant mix design ratio for the mortar mixture, the influence of the water-to-binder (W/B) ratio is essential to activate the geopolymerization and control the microstructural properties of the mortar. Reduction in porosity and drying shrinkage depends on excessive hydration product content in alkali-activated binder technology. When the water is added, the chemical reaction known as hydration is initiated and produces the final hardened material products by forming the calcium silicate hydrate (*C*–S–H) gels to fill the open pores to form a solid microstructure. A lower W/B ratio ensures a low porosity level of mortar sample G3 (W/B of 0.30), with 16.7%, followed by mortar sample G2, with 17.4%, and mortar sample G1 recorded the highest porosity level at 18.9%. At a lower porosity level, Mix G3 recorded 54 MPa, the utmost recorded strength for 28-d age. Furthermore, at 56 days, the compressive strength continued to develop up to 63 MPa and recorded the highest pull-off bonding strength of 2.21 MPa. This understanding explained the intercorrelation between porosity level and mechanical strength to control the shrinkage level of the mortar.

A lower porosity level ensures that the hardened mortar has a compact microstructure and fewer pores to avoid intrusion of water,

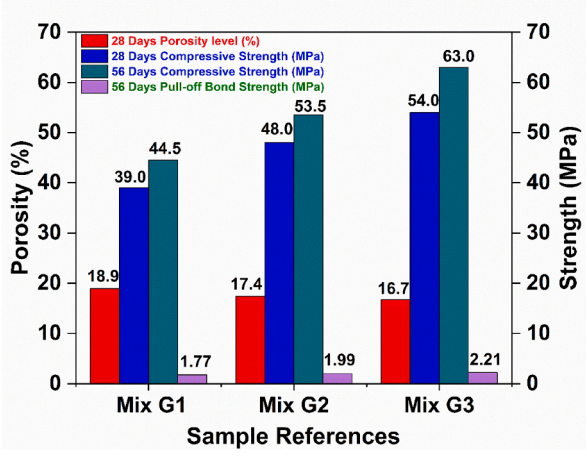

Fig. 5. Porosity level vs compressive strength of one-part AAMs mortar.

gas, or other potential chemical attacks helps to increase the mechanical strength on both compressive strength's development at 28 days of curing age uninterruptedly to a last 56 days of age as reported in this study. In addition, FA consists of rich silica content that improves the process of dissolution and polymerization, contributing to low porosity microstructures [37]. Moreover, the input of Si is more efficient with low water content [38]. As a result, the pull-off bond strength remains consistent above 2.0 MPa for of mortar sample with the lowest W/B ratio (mortar sample G3) encountering the shrink-hardened mortar at 56 days of age and shows the water content effect on monitoring drying shrinkage and expansion behaviour (by means of pull-off bond strength result) subsequently complies with structural repair products of class R4 – EN1504-3 standard. These findings also confirmed that hardened mortar with a low porosity level corresponds to the lowest drying shrinkage and better mechanical strength [39].

3.5. Scanning Electron Microscope (SEM)

The microstructure of one-part alkali-activated materials was studied using Scanning Electron Microscope (SEM). The hardened mortar was produced with different percentages of mix composition consisting of fly ash which contains 25% of total precursors weight, 5% slag and 70% ordinary Portland cement as main aluminosilicate precursors, which is donated to the densified microstructure of the mortar. Few spots were captured for the SEM images of mortar samples G2 and G3, and only images with overall textures, i.e., pores, cracks, and compacted surfaces, are shown in this report to understand the microstructures of the hydrated particles. Fig. 6 and Fig. 7 showed that both SEM images for samples G2 (Fig. 6a) and G3 (Fig. 7a) are well hydrated in general, compact and homogenous with new calcium sodium aluminosilicate hydrated gels on their surfaces. Interestingly, using a 1.8% dry activator type of potassium carbonate still contributes to lesser unreacted calcium as s sign of effective chemical reaction between precursors, admixtures, and low alkali activators with appropriate water content.

Nevertheless, the morphology of the two mortar samples is similar from the perspective of porosity and aggregate-mortar interface, including some unreacted particles pattern. Both images also depict the micropores and microcracks marks but exhibit a glass-like surface representing the geopolymeric gel. The microcracks frequently occur due to irregular shrinkage forces among gels and particles throughout the drying process, besides the loss of water in gels [1]. SEM images zoomed in to 20 μm, focusing on spherically shaped areas, revealed that sample G2 has a less spherical structure than sample G3, which consists of more spherical spots, as shown in Figs. 6b and 7b However, it can also observe in this image that the pores of sample G3 are more prominent, which supports the pore structure distribution result for the mortar sample with a low water content of W/B ratio of 0.30, has higher average pore diameters than the mortar sample G2.

3.6. Microstructural development

All raw materials used in this study, from aluminosilicate precursors, alkali activators and solid admixtures, have good reactivity, are chemically stable in reaction and are well dissolved when in contact with water. Optimum water-to-binder content ensures the hydrolysis of all these solid activators takes part to facilitate the network breakdown of solid precursors. Dissolved ions would undergo gelation and condensation, as reported by Lv et al. [40]. A higher Si/Al ratio obtained from fly ash is beneficial to encourage low porosity microstructure, improving sample compactness for better mechanical strength [37,41,42]. Adding GGBFS/OPC further supplies calcium and balances the short supply in FA, assisting in stronger chemical bonds for hydration products.

A higher volume of OPC is beneficial to wrap the water in the cement particles and reduce the amount of free water in the fresh mortar mixes, subsequently increasing adequate solid volume friction for better compactness and leading to higher mechanical strength [27]. Three exothermic reactions after the addition of water in one-part AAMs are the dissolution of raw materials (NaOH and hydration of CaO), bond breaking (attack of OH^- on *Si*–O and Al–O bonds) and release of Ca, Si and Al and formation of gels via polymerization as reported by Ref. [8]. Unreacted particles decrease in quantity with a longer curing time and a higher dosage of alkali activator in the system. However, lower alkali activator dosages were used in this experiment. Only 70% of OPC content was used in the mix, yet it contributed to a more compact and less porous structure and less unreacted fly ash particles, as agreed by Ref. [7]. Fly ash particles composed of microspheres, amorphous alumina and/or silica-rich materials can be dissolved in alkalinity [43]. The spherical particles will be embedded in the form of material and contribute to better mechanical strength over time. Spherical structures are spotted in this study's SEM image, commonly known as the unreacted fly ash component, in agreement with Azevedo et al. [10] on the fact that fly ash particles remain even after contact with alkaline materials in all curing periods, probably caused by low alkaline reactivity. In this report, mortar sample G3, which has more spherical shape particles, recorded growth compressive strength from 7 days (39.0 MPa) to 28 (54.0 MPa) and 56 days (63.0 MPa) of curing age and retained its pull-off bond strength at an

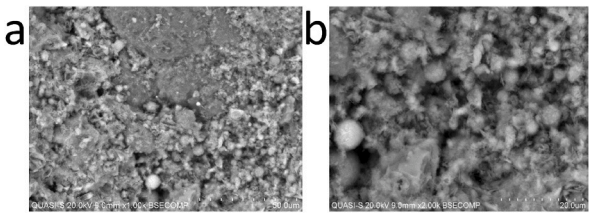

Fig. 6. SEM Image of sample G2 (a) Overview and (b) Spherical structure.

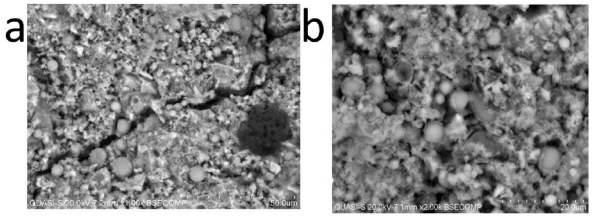

Fig. 7. SEM Image of sample G3 (a) Overview and (b) Spherical structure.

average of above 2.0 MPa at 56 days of age. It proves that the spherical/unreacted fly ash particles were still experiencing the geopolymerization process after 28 days of age. It was also helpful to understand that some unreacted particles are inherited from the parent material of hydration products, as suggested by Ref. [29].

A compact structure shows good adhesion and explains the increase in mechanical strength of the mortar. The compaction of microstructures improved with a more extended curing period, confirming the increment of strength over time for both mortar [39] samples as recorded in the compressive strength test at 7, 28 and 56 days of curing age in this report. Therefore, the unreacted particles in the SEM images may act as micro fillers in the mixes and improve their compactness. Both images have shown microcracks spots. Although a line of microcracks is more visible in the mortar sample, the G3 image may indicate the loss of water [44] or temperature cracks due to the heat generated from the reaction between the sodium oxide of the alkali activator and water [15] and uneven shrinkage forces between derivatized gel and the particles. All take place during the curing period [1]. The cracks' formation could degrade the mechanical performance of the mortar over time. Though, Almalkawi et al. [29] reported other factors on why microcracks could appear or get visible areas due to the drying process of the specimen for Scanning Electron Microscope (SEM). The clear microcracks image proves that the mortar sample G3 (19.52 nm) has a higher average pore diameter than G2 (18.21 nm), in line with the MIP test result for pore structure distribution. It was reported that an 8% solid activator (by weight %) used to activate FA/GGBFS one-part AAMs only achieved about 30 MPa at 28 days of curing age, where more unreacted particles were observed in SEM image [45]. In contrast, as the low alkaline level of the alkali activator (1.6% K_2CO_3 by weight) used in this study observed, fewer unreacted particles were found on both SEM images for samples G2 and G3. Yet, they achieved significant compressive strength value, proving that this type of mortar samples initiated with a low amount of alkali activator have substantial potential to improve the current technology of one-part AAMs.

Alkali activated materials concept is much contributed by the dissolution of aluminosilicate precursors with the formation of geopolymeric gels of low atomic order favourable for hardened materials cementing properties [10]. The preparation of samples in this study was conducted under controlled temperatures and not exposed to high temperatures that could trigger dissolution. On the other hand, the geopolymerization begins with the calcium reacting with potassium carbonate to create *C*–S–H gels, consequently elevating the pH of the alkaline mix and reducing water content. Under an alkaline environment, the dissolution of aluminosilicate precursors was initiated, subsequently ameliorating polycondensation and polymerization reactions for the hardening process. The precipitated compounds and geopolymeric gels of *N*-A-*S*-H and *C*-A-*S*-H contributed strength and remained to develop higher over time as the geopolymerization continued.

On the contrary, at a higher temperature level of 65 Celsius, the dissolution of aluminosilicate precursors quickens to form geopolymeric compounds at an early age for higher early strength [18]. Still, it may also cause incomplete dissolution of aluminosilicate compounds given that geopolymeric slurries could cover the undissolved precursor, limiting further dissolution besides water evaporation and excessive shrinkage problem creating more cracks and pores and finally decreasing the strength of the mortar. Samarakoon et al. [11] reported that at the early age of curing, the hydration product for one-part AAMs is mainly composed of *C*-A-*S*-H type gels. However, the reaction products are moreover *C*–S–H dominant due to higher reactivity, and easier discharge of calcium ions can be found as early as 1 day of curing age. At the same time, the other portion of silicon and aluminium remains unreacted on the surface of the reacted phase. After 28 days, calcium content will be reduced. Still, silicon involvement in hydration products is increased because higher portions of fly ash could promote zeolite formation at the later curing stage when the composition of the binder is SiO_2-rich; the

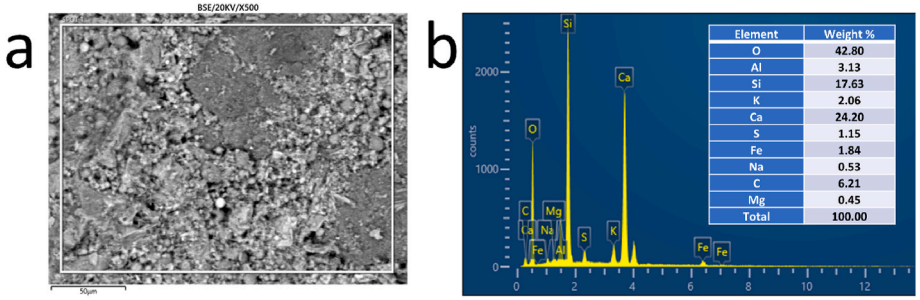

Fig. 8. SEM-EDX of sample G2 (a) Image and (b) Weight (%).

incorporation of Na is also favoured, later confirming the co-existence between *C*-A-*S*-H and *N*-A-*S*-H with a potential cross-linked structure of *C*-(N)-A-*S*-H type gels at subsequent curing. In this report an optimum W/B of 0.30 effectively initiate the chemical reaction and created *C*-(N)-A-*S*-H type gels which assist the hardened mortar with low porosity level not only able to resist leaching through its open pores but also offer more stable geopolymeric link gels against chemical attacks and maintaining its mechanical strength, beneficial for one-part AAMs long-term effectiveness.

3.7. Characterization of reaction products using – SEM-EDX

The difference in the surfaces of the hybrid one-part alkali-activated mortar activated by different water-to-cement ratios was further investigated by the chemical element composition at a specific area using the EDX. The resulting SEM images at 28 days of curing with the corresponding EDX maps at 28 days of curing are shown in Fig. 8a – Fig. 9a. During the curing period, microstructures of all mortar samples become dense by reducing micro-pores, reflecting compressive strength development with time due to highly compacted and low porosity levels [46]. The formation and spatial distribution for both mortar samples consistently depict a well-blended elemental distribution for the formation of homogenous and dense microstructure [11]. The reaction process in AAMs requires a few steps starting with the dissolution of Ca, Si and Al from aluminosilicate precursors, a re-orientation process, re-interaction and condensation to develop the strength [34]. Additionally, the chemical compositions of Ai/Al and/or Na/Si atomic ratios and K/Al molar ratio are beneficial to determining the mechanical properties of the AAMs, which are in connection with its products dissolution rate [21,43]. It was explained in a past report on forming *C*-A-*S*-H gels that were regarded as aluminium substituted *C*–S–H phase in AAMs technology. Aluminium (Al) in *C*-A-*S*-H functioned in bridging tetrahedral sites. Still, the different extent was restricted by chemical limitations due to a defect of the tobermorite structure [40]. The overall constituent of geopolymerization products for mortar samples G2 and G3 have consisted of newly formed hybrid geopolymeric products *N*-A-*S*-H gels co-existing with *C*-A-*S*-H gels. New hydration products of *C*-(N)-A-*S*-H type gel were confirmed using EDX point analysis on dominant elemental phases in the reacted cement binder, mainly silicon, calcium, aluminium, and sodium.

The higher weight percentage of Ca/Si found in sample G3 (Fig. 9b) than in sample G2 (Fig. 8b) is a sign of a higher Ca/Si molar ratio beneficial for the early formation of *C*–S–H. Askarian et al. [7] reported that CaO to SiO_2 (Ca/Si) decreases with decreasing OPC content in geopolymer mixes. Mixing with a higher Ca/Si ratio is beneficial to form *C*–S–H gels, which can improve the early strength of mortar. The combination of OPC and FA/GGBFS creates different nature of *C*–S–H gels (stronger bond) compared to the typical *C*–S–H gels formed in OPC alone. Luukkonen et al. [47] reported that Ca/Si increases when sodium lignosulfonate – superplasticizer introduced in the mortar with Ca^{2+} reaction from lignosulfonate could facilitate the dissolution of slag to increase the amount of calcium and likely to increase the compressive strength of mortar. It is worth noting that the roles of SP admixtures used as part of the mix design reacted well in assisting the dissolution process when a W/B ratio of 0.30 was added to ensure the efficiency of 30% OPC total weight reduction in the mixes and replaced with FA and slag yet still has a comparable Ca/Si ratio with sole OPC precursor.

4. Conclusion

The one-part AAMs experienced coarser pore fractions above 20 nm, affecting their durability and mechanical strength compared to the two-part counterpart. A larger pore diameter will cause higher porosity and be prone to chemical attacks, especially when the location is exposed to adverse climate and temperature. This report established the effect of adequate water content through a water-to-binder (W/B) ratio to improve one-part alkali-activated mortar. Unlike the past report on hybrid one-part AAMs, the mortar samples in this study were activated with only 1.8% alkali activator and composed of 70% OPC with 25% FA and 5% GGBFS as main precursors sources. Three types of admixtures were added to stabilize the mortar's physical properties. As a result, the W/B ratio of 0.30 exhibit the best overall performance in the fresh and hardened mortar state. A lower W/B ratio also contributes to the low porosity level of hardened mortar by controlling its pore structure. It subsequently overcame the shortfall of the current one-part technology and achieved the aim of this study. The mix design formulation is now completed for the production of geopolymer binder as per class R4 – EN1504-3 standard for structural concrete repair materials applications.

Furthermore, this mix design formulation confirms it successfully replaces 30% of OPC volume with industrial by-product precursors as the first step in diminishing reliance on the OPC and another effort to reduce clinker production, reusing waste products, and subsequently control the CO_2 emissions. This report also summarizes that the hardening mechanism and microstructures of hybrid one-part alkali-activated mortar changed significantly when the mortar was composed of different water-to-binder ratios, producing different mechanical strengths at early and later stages affecting the pore structure distribution. The ongoing geopolymerization process over time encourages continuous pore structure refinements, which is essential to control the total porosity level and guarantee mechanical strength growth beyond 28 days of curing age. A significantly lower porosity value below 20% was recorded for mortar samples G3, which is beneficial for controlling the drying shrinkage effect.

Nevertheless, the SEM images of the mortar specimen at 28 days of curing age for both mortar samples G2 and G3 show almost identical structures and similar final products. The only differences brought by different W/B ratios were in the amount of reacted geopolymer gels (dense, homogenous, glass-like surface)/unreacted precursors (spherical structures) and micropores/microcracks elements. Unlike the conventional one-part AAMs, where the dissolution of precursors is not completed under low alkaline reactivity, leading to more unreacted particles, the mortar samples G2 and G3, on the other hand, have dense, compact, and homogenous reacted geopolymer gels.

Apart from the influence of water content discussed in this report, another finding showed that the usage of a low alkali activator reacted well with all precursors, in addition to the optimum content of solid admixtures for the geopolymerization process and offered

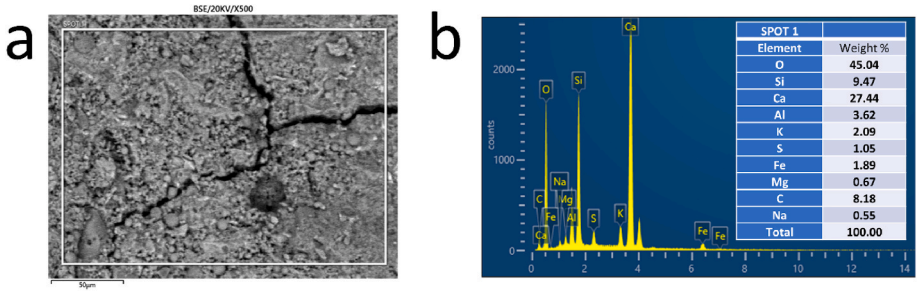

Fig. 9. SEM-EDX of sample G3 (a) Image and (b) Weight (%).

reliable mechanical and microstructural properties for the hardened mortar. Although the hybrid one-part alkali-activated mortar has a significantly low porosity level and consistent mechanical strength, a future study must focus on the stability of its pore structures against severe environmental conditions and chemical attacks in a different climate to ensure its durability and efficacy for long-term application.

Author contribution statement

Eddy Yusslee: Conceived and designed the experiments; Performed the experiments; Analyzed and interpreted the data; Contributed reagents, materials, analysis tools or data; Wrote the paper.

Sherif Beskhyroun: Contributed reagents, materials, analysis tools or data.

Funding statement

This research did not receive any specific grant from funding agencies in the public, commercial, or not-for-profit sectors.

Data availability statement

No data was used for the research described in the article.

Declaration of interest's statement

The authors have no conflicts of interest to declare.

Acknowledgements

Special thanks to Engineering New Zealand (ENZ), The Association of German Engineers (VDI) and the Sabah Public Service Department, Malaysia, which contributed to the outcome of this experiment.

References

[1] C. Liu, X. Yao, W. Zhang, Controlling the setting times of one-part alkali-activated slag by using honeycomb ceramics as carrier of sodium silicate activator, Construct. Build. Mater. 235 (2020), 117091, https://doi.org/10.1016/j.conbuildmat.2019.117091.

[2] H.A. Khan, M.S.H. Khan, A. Castel, J. Sunarho, Deterioration of alkali-activated mortars exposed to natural aggressive sewer environment, Construct. Build. Mater. 186 (2018) 577–597, https://doi.org/10.1016/j.conbuildmat.2018.07.137.

[3] E. Hany, N. Fouad, M. Abdel-Wahab, E. Sadek, Compressive strength of mortars incorporating alkali-activated materials as partial or full replacement of cement, Construct. Build. Mater. 261 (2020), 120518, https://doi.org/10.1016/j.conbuildmat.2020.120518.

[4] S.A. Bernal, J.L. Provis, Durability of alkali-activated materials: progress and perspectives, J. Am. Ceram. Soc. 97 (4) (2014) 997–1008, https://doi.org/10.1111/jace.12831.

[5] T. Phoo-Ngernkham, S. Hanjitsuwan, L.Y. Li, N. Damrongwiriyanupap, P. Chindaprasirt, Adhesion characterization of Portland cement concrete and alkali-activated binders, Adv. Cement Res. 31 (2) (2019) 69–79, https://doi.org/10.1680/jadcr.17.00122.

[6] P. Perumal, et al., High strength one-part alkali-activated slag blends designed by particle packing optimization, Construct. Build. Mater. 299 (2021), 124004, https://doi.org/10.1016/j.conbuildmat.2021.124004.

[7] M. Askarian, Z. Tao, G. Adam, B. Samali, Mechanical properties of ambient cured one-part hybrid OPC-geopolymer concrete, Construct. Build. Mater. 186 (2018) 330–337, https://doi.org/10.1016/j.conbuildmat.2018.07.160.

[8] T. Luukkonen, Z. Abdollahnejad, J. Yliniemi, P. Kinnunen, M. Illikainen, One-part alkali-activated materials: a review, Cement Concr. Res. 103 (October) (2018) 21–34, https://doi.org/10.1016/j.cemconres.2017.10.001.

[9] T. Yang, et al., Effects of calcined dolomite addition on reaction kinetics of one-part sodium carbonate-activated slag cements, Construct. Build. Mater. 211 (2019) 329–336, https://doi.org/10.1016/j.conbuildmat.2019.03.245.

[10] A. Galvão Souza Azevedo, K. Strecker, Kaolin, fly-ash and ceramic waste based alkali-activated materials production by the 'one-part' method, Construct. Build. Mater. 269 (2021), https://doi.org/10.1016/j.conbuildmat.2020.121306.

[11] M.H. Samarakoon, P.G. Ranjith, W.H. Duan, V.R.S. De Silva, Properties of one-part fly ash/slag-based binders activated by thermally-treated waste glass/NaOH blends: a comparative study, Cem. Concr. Compos. 112 (2020), 103679, https://doi.org/10.1016/j.cemconcomp.2020.103679. December 2019.

[12] W. Chen, R. Peng, C. Straub, B. Yuan, Promoting the performance of one-part alkali-activated slag using fine lead-zinc mine tailings, Construct. Build. Mater. 236 (2020), 117745, https://doi.org/10.1016/j.conbuildmat.2019.117745.
[13] V.A. Nunes, P.H.R. Borges, C. Zanotti, Mechanical compatibility and adhesion between alkali-activated repair mortars and Portland cement concrete substrate, Construct. Build. Mater. 215 (2019) 569–581, https://doi.org/10.1016/j.conbuildmat.2019.04.189.
[14] X. Ke, S.A. Bernal, N. Ye, J.L. Provis, J. Yang, One-part geopolymers based on thermally treated red Mud/NaOH blends, J. Am. Ceram. Soc. 98 (1) (2015) 5–11, https://doi.org/10.1111/jace.13231.
[15] M. Askarian, Z. Tao, B. Samali, G. Adam, R. Shuaibu, Mix composition and characterization of one-part geopolymers with different activators, Construct. Build. Mater. 225 (2019) 526–537, https://doi.org/10.1016/j.conbuildmat.2019.07.083.
[16] E. Yusslee, S. Beskhyroun, The potential of one-part alkali-activated materials (AAMs) as a concrete patch mortar, Sci. Rep. 12 (1) (2022), 15902, https://doi.org/10.1038/s41598-022-19830-0.
[17] S. Haruna, B.S. Mohammed, M.M.A. Wahab, M.S. Liew, Effect of paste aggregate ratio and curing methods on the performance of one-part alkali-activated concrete, Construct. Build. Mater. 261 (2020), 120024, https://doi.org/10.1016/j.conbuildmat.2020.120024.
[18] S.F.A. Shah, B. Chen, S.Y. Oderji, M.A. Haque, M.R. Ahmad, Improvement of early strength of fly ash-slag based one-part alkali activated mortar, Construct. Build. Mater. 246 (2020), 118533, https://doi.org/10.1016/j.conbuildmat.2020.118533.
[19] T. Luukkonen, Z. Abdollahnejad, J. Yliniemi, P. Kinnunen, M. Illikainen, One-part alkali-activated materials: a review, Cement Concr. Res. 103 (2018) 21–34, https://doi.org/10.1016/j.cemconres.2017.10.001. October 2017.
[20] Y. Alrefaei, Y.S. Wang, J.G. Dai, The effectiveness of different superplasticizers in ambient cured one-part alkali activated pastes, Cem. Concr. Compos. 97 (2019) 166–174, https://doi.org/10.1016/j.cemconcomp.2018.12.027. September 2018.
[21] A. Mobili, F. Tittarelli, H. Rahier, One-part alkali-activated pastes and mortars prepared with metakaolin and biomass ash, Appl. Sci. 10 (16) (2020), https://doi.org/10.3390/app10165610.
[22] M. Liu, H. Wu, P. Yao, C. Wang, Z. Ma, Microstructure and macro properties of sustainable alkali-activated fly ash mortar with various construction waste fines as binder replacement up to 100, Cem. Concr. Compos. 134 (2022), 104733, https://doi.org/10.1016/j.cemconcomp.2022.104733. June.
[23] M. Liu, C. Wang, H. Wu, D. Yang, Z. Ma, Reusing recycled powder as eco-friendly binder for sustainable GGBS-based geopolymer considering the effects of recycled powder type and replacement rate, J. Clean. Prod. 364 (2022), 132656, https://doi.org/10.1016/j.jclepro.2022.132656. June.
[24] S. Candamano, P. De Luca, P. Frontera, F. Crea, Production of geopolymeric mortars containing forest biomass ash as partial replacement of metakaolin, Environ. - MDPI 4 (4) (2017) 1–13, https://doi.org/10.3390/environments4040074.
[25] R.H. Geraldo, O.G. Teixeira, S.R.C. Matos, F.G.S. Silva, J.P. Gonçalves, G. Camarini, Study of alkali-activated mortar used as conventional repair in reinforced concrete, Construct. Build. Mater. 165 (2018) 914–919, https://doi.org/10.1016/j.conbuildmat.2018.01.063.
[26] O.G. Teixeira, R.H. Geraldo, F.G. da Silva, J.P. Gonçalves, G. Camarini, Mortar type influence on mechanical performance of repaired reinforced concrete beams, Construct. Build. Mater. 217 (2019) 372–383, https://doi.org/10.1016/j.conbuildmat.2019.05.035.
[27] L. Li, J.X. Lu, B. Zhang, C.S. Poon, Rheology behavior of one-part alkali activated slag/glass powder (AASG) pastes, Construct. Build. Mater. 258 (2020), 120381, https://doi.org/10.1016/j.conbuildmat.2020.120381.
[28] A. Palomo, O. Maltseva, I. Garcia-Lodeiro, A. Fernández-Jiménez, Portland versus alkaline cement: continuity or clean break: 'A key decision for global sustainability, Front. Chem. 9 (2021) 1–28, https://doi.org/10.3389/fchem.2021.705475. October.
[29] A.T. Almalkawi, S. Hamadna, P. Soroushian, One-part alkali activated cement based volcanic pumice, Construct. Build. Mater. 152 (2017) 367–374, https://doi.org/10.1016/j.conbuildmat.2017.06.139.
[30] E. Yusslee, S. Beskhyroun, Performance evaluation of hybrid one-Part Alkali activated materials (AAMs) for concrete structural repair, Buildings 12 (11) (2022), https://doi.org/10.3390/buildings12112025.
[31] R. Robayo-Salazar, C. Jesús, R. Mejía de Gutiérrez, F. Pacheco-Torgal, Alkali-activated binary mortar based on natural volcanic pozzolan for repair applications, J. Build. Eng. 25 (2019), 100785, https://doi.org/10.1016/j.jobe.2019.100785. April.
[32] L. Coppola, et al., The combined use of admixtures for shrinkage reduction in one-part alkali activated slag-based mortars and pastes, Construct. Build. Mater. 248 (2020), 118682, https://doi.org/10.1016/j.conbuildmat.2020.118682.
[33] I.L. Tchetgnia Ngassam, P. Arito, H. Beushausen, A new approach for the mix design of (patch) repair mortars, African J. Sci. Technol. Innov. Dev. 10 (3) (2018) 259–265, https://doi.org/10.1080/20421338.2018.1452845.
[34] B. Yang, J.G. Jang, Environmentally benign production of one-part alkali-activated slag with calcined oyster shell as an activator, Construct. Build. Mater. 257 (2020), 119552, https://doi.org/10.1016/j.conbuildmat.2020.119552.
[35] S. Kramar, A. Šajna, V. Ducman, Assessment of alkali activated mortars based on different precursors with regard to their suitability for concrete repair, Construct. Build. Mater. 124 (2016) 937–944, https://doi.org/10.1016/j.conbuildmat.2016.08.018.
[36] M. Almakhadmeh, A.M. Soliman, Effects of mixing water temperatures on properties of one-part alkali-activated slag paste, Construct. Build. Mater. 266 (2021), 121030, https://doi.org/10.1016/j.conbuildmat.2020.121030.
[37] M.N. Qureshi, S. Ghosh, Effect of Si/Al ratio on engineering properties of alkali-activated GGBS pastes, Green Mater. 2 (3) (2014) 123–131, https://doi.org/10.1680/gmat.14.00001.
[38] E. Pereira, E. Br, A. Resende, M.H.F. De Medeiros, L.C. Meneghetti, Chloride accelerated test: influence of silica fume, water/binder ratio and concrete cover thickness Ensaio acelerado por cloretos: efeito da sílica ativa, relação água/aglomerante e espessura de cobrimento do concreto Chloride accelerated test: influence, IBRACON Struct. Mater. J. • 2013 • 6 (4) (2013) 4.
[39] H.A. Abdel-Gawwad, A.M. Rashad, M. Heikal, Sustainable utilization of pretreated concrete waste in the production of one-part alkali-activated cement, J. Clean. Prod. 232 (2019) 318–328, https://doi.org/10.1016/j.jclepro.2019.05.356.
[40] W. Lv, Z. Sun, Z. Su, Study of seawater mixed one-part alkali activated GGBFS-fly ash, Cem. Concr. Compos. 106 (2020), 103484, https://doi.org/10.1016/j.cemconcomp.2019.103484. June 2019.
[41] S. Thokchom, K.K. Mandal, S. Ghosh, Effect of Si/Al ratio on performance of fly ash geopolymers at elevated temperature, Arabian J. Sci. Eng. 37 (4) (2012) 977–989, https://doi.org/10.1007/s13369-012-0230-5.
[42] Y. Wang, et al., Effects of Si/Al ratio on the efflorescence and properties of fly ash based geopolymer, J. Clean. Prod. 244 (2020), 118852, https://doi.org/10.1016/j.jclepro.2019.118852.
[43] H. Choo, S. Lim, W. Lee, C. Lee, Compressive strength of one-part alkali activated fly ash using red mud as alkali supplier, Construct. Build. Mater. 125 (2016) 21–28, https://doi.org/10.1016/j.conbuildmat.2016.08.015.
[44] T. Luukkonen, Z. Abdollahnejad, J. Yliniemi, P. Kinnunen, M. Illikainen, Comparison of alkali and silica sources in one-part alkali-activated blast furnace slag mortar, J. Clean. Prod. 187 (2018) 171–179, https://doi.org/10.1016/j.jclepro.2018.03.202.
[45] S. Yousefi Oderji, B. Chen, M.R. Ahmad, S.F.A. Shah, Fresh and hardened properties of one-part fly ash-based geopolymer binders cured at room temperature: effect of slag and alkali activators, J. Clean. Prod. 225 (2019) 1–10, https://doi.org/10.1016/j.jclepro.2019.03.290.
[46] H.A. Abdel-Gawwad, S.R.V. García, H.S. Hassan, Thermal activation of air cooled slag to create one-part alkali activated cement, Ceram. Int. 44 (12) (2018) 14935–14939, https://doi.org/10.1016/j.ceramint.2018.05.089.
[47] T. Luukkonen, Z. Abdollahnejad, K. Ohenoja, P. Kinnunen, M. Illikainen, Suitability of commercial superplasticizers for one-part alkali-activated blast-furnace slag mortar, J. Sustain. Cem. Mater. 8 (4) (2019) 244–257, https://doi.org/10.1080/21650373.2019.1625827.